

# Gone Fishin'

Douglas Martin  
Robert A. Moody  
Woon (Larry) Wong  
Pomona College  
Claremont, CA 91711

Advisor: Ami Radunskaya

## Abstract

We develop a method to measure the ambient field, using directional transducers and programmable electronic delay circuitry, so that we can determine the ambient sound pressure for a given cell in three-dimensional space.

We discuss the expected observations from the interaction of the target object and the ambient field, and the associated limitations of our method.

We conducted a simple experiment that verified that our approach worked in an anechoic environment (outdoors), and we argue that the results should generalize to the underwater environment.

We show how our method produces data sufficient to reconstruct object size, position, and velocity, and we present the algorithms required to accomplish this reconstruction. We discuss the advantages and problems associated with various reference frequencies, and methods to optimize the technique. Finally, we present a model of the anticipated characteristic performance of our method.

## Ambient Sounds

(All of the background information in this section comes from Naval Sea Systems Command [1984].)

Ambient noise in the ocean can be classified into background or continuous noise, which is present for extended durations of time, and intermittent sounds or noises generated at random intervals for essentially random durations.

The background is comprised primarily of wind-based noises, noises from commercial shipping, and other similar human-made sources. Some seismic noise is present, particularly at lower frequencies.

Intermittent noises can be further divided into biological and nonbiological. Multi-watt whale sounds range from low-frequency moans to high frequency clicks and have a frequency range of at least 2 Hz–60 kHz.

Intermittent nonbiological noise include the rain, earthquakes, explosions, and volcanoes. Although there is some additional noise generated by the surf, the poor propagation characteristics of the shallow water in which such noise

is generated cause a rapid decay; thus these sounds do not appear to contribute heavily to the ambient field in the deep sea. The contributions of rain, earthquakes, and volcanoes are continuous enough for us to group them under the general heading “background noise,” since they can reasonably be expected to have periods vastly larger than our scanning period. Explosions are, from our perspective, an overwhelming problem.

Studies have confirmed both the directionality and spatial coherence characteristics of ambient sound, both background and intermittent [Urick 1983]. Shipping noise, which is primarily in the 100 Hz range, tends to travel horizontally and at low angles. Wind noise, dominant in the higher frequencies (1,000 Hz and above), travels over relatively direct paths and tends to arrive at angles between 45° and 80° relative to the surface.

## Sonar

Active sonar involves generating sound and determining the bearing and distance of the target object by measuring the time that it takes the echo to return to elements of the sensor array. In passive sonar, the target is the source of the detected sound. In both cases, the detected sound is effectively radiated from a point source, the target. The parameters that relate to the efficacy of passive sonar are [Urick 1983]:

SL, source level;

DI, receiving directivity index;

DT, detection threshold;

TL, transmission loss attributable to the medium; and

NL, ambient noise level.

These are related through the passive sonar equation:

$$SL - TL = NL - DI + DT.$$

Since we are detecting the noise directly and attempting to measure the absence of noise along a particular directional axis, we reverse the SL and NL terms. Thus, we attempt to locate the loud fields and thereby detect the lower-power fields via elimination. Since we predict extremely small deviations in the source and noise levels, we depend quite heavily on the directivity index as the parameter that enables us to construct an effective system.

## Acoustic Impact of Submarine

At low speeds or at rest, the submarine will look like a hole in the noise field. Since the ambient field is homogeneous (that is, same intensity from any direction), the submarine appears as an absorber. It reflects sound waves; sound coming toward the observer from the other side of the submarine is deflected away from the observer, while sound coming from the same side as the observer is reflected towards the observer. Both these sound waves have the same intensity, so the net effect is that the submarine will look the same as the ambient field but reduced by a reflection coefficient. Similar considerations apply to sound coming at off-axis angles. See **Figure 1**, in which  $A$ ,  $B$ ,  $C$ , and  $D$  are incident ambient sound waves of equal intensity, with  $aA$ ,  $aB$ ,  $aC$ , and  $aD$  being their reflections from the submarine, for reflection coefficient  $a$ . Thus, the submarine masks  $A$  and  $B$  from the detector but reflects  $aC$  and  $aD$  toward the detector. Since each wave is of equal intensity, the effect of the submarine is to change the ambient field coming from behind it by a factor of  $a$ .

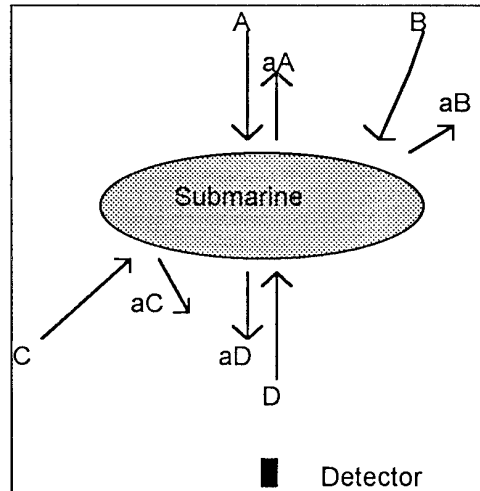


**Figure 1.** Effect of a submarine on ambient noise.

The formula for the reflection coefficient for a liquid-liquid boundary is

$$a = \left( \frac{R_2 - R_1}{R_2 + R_1} \right)^2,$$

where  $R_2$  and  $R_1$  are the acoustic impedances of the reflecting medium and the incident medium [Tucker and Gazey 1966, 91]. The liquid-solid reflection coefficient is far more complicated and, for our purposes, not significantly different. For the case of steel and water, we have  $R_2 = 3,900,000$  and  $R_1 = 154,000$  [Horton 1957, 26], which give  $a = .854$ . However, practical submarine designs minimize  $a$  to avert sonar detection; so a more likely value of  $a$  is probably about .1.

We can predict the difference in the ambient field from the submarine's presence. For ambient field intensity  $I_a$ , the reflected intensity is  $I_r = aI_a$ .

So the difference in decibels between the reflected intensity and the ambient intensity is

$$20 \log I_a - 20 \log(aI_a) = 20 \log I_a - 20(\log a + \log I_a) = -20 \log a.$$

For a steel submarine with no noise reflection damping, the difference is 1.37 dB; for a more realistic submarine, the difference is 20 dB; and for the perfectly noiseless submarine, the difference is infinite in dB, which corresponds to the entire ambient noise level (that is, for ambient noise level of 60 dB, the difference between the submarine and the ambient noise level is also 60 dB). Using a hydrophone (underwater microphone) array, we can detect the lower level of the ambient noise field and know that a submarine is there.

## Microphones, Hydrophones, and Other Transducers

Most of the literature about hydrophones implies their use in linear arrays, generally either bottom-fixed or fixed to a vertical line that is stretched by a weight affixed to the sunken end of the line. Sonar receptors are mounted in either circular or cylindrical arrays with bearing determined by sound arrival times. In both of these general cases, the hydrophones used are omnidirectional, an undesirable feature for our purposes. Albers [1965] and Horton [1957] describe methods to determine source location using either linear or planar arrays of omnidirectional hydrophones or hydrophones with cardioid response patterns

There are three alternative techniques for limiting microphone pickup patterns that are vastly superior to reliance on a simple cardioid pattern.

- The “tuned port” microphone tube (see **Figure 2**) cancels off-axis sound by allowing it to arrive at the microphone element via several separate paths, slightly out of phase with each other, so that the off-axis sound interferes with itself, thus canceling the unwanted sound.

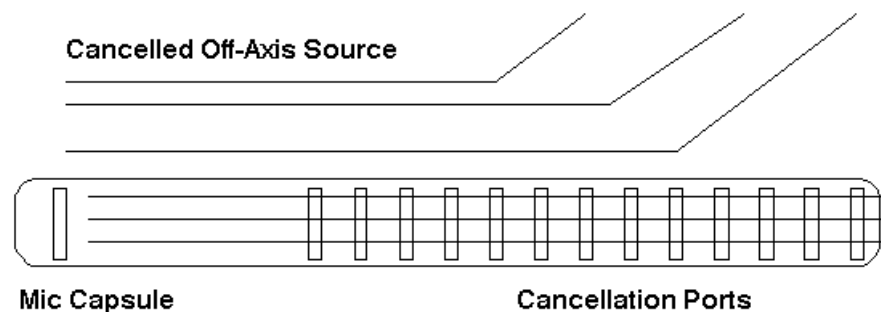


**Figure 2.** Shotgun tuned port microphone.

- A parabolic reflector selectively increases the impact of head-on waves with respect to the microphone element. The parabolic reflector involves several problems with water flow that we are not prepared to address.

The frequency limitations of both techniques present tradeoffs to various aspects of the model. Higher frequencies are absorbed at a greater rate in water (or any other medium), and as a result, the effective distance of the method will be adversely affected by choosing higher frequencies. Conversely, lower frequencies are less directional, have longer wavelengths (and so are less selective), and are much more difficult to deal with when attempting to decrease the beamwidth of the sound pickup pattern.

- “Pressure zone microphones” (PZM), also known as boundary microphones, are basically condenser microphone elements located close to a planar reflective boundary. Increasing the size of the boundary decreases the frequency at which the microphone becomes directional, in accordance with the formula  $F = 188/D$ , where  $F$  is the frequency at which the microphone becomes directional and  $D$  is the boundary dimension in feet (assuming a square boundary). Thus, a  $2 \times 2$ -ft boundary results in directionality at or above 94 Hz and a supercardioid response (rejection greater than 12 dB at or over  $30^\circ$  off-axis) at frequencies around 500 Hz [Bartlett 1991]. By using two panels with two microphones, an extremely directional response pattern can be achieved as a result of phase cancellation. Using  $2 \times 2$ -ft panels at an angle of  $60^\circ$  to each other, the on-axis sensitivity angle is approximately  $7.5^\circ$  (see **Figure 3**). Although this method is not mentioned in the underwater literature, we believe that we can achieve beam widths of arbitrarily narrow widths (with a  $5^\circ$  arc probably representing a practical minimum) by using this microphone design, as adapted to underwater use, in conjunction with Horton’s phase-delay methods [1957, 247–248].

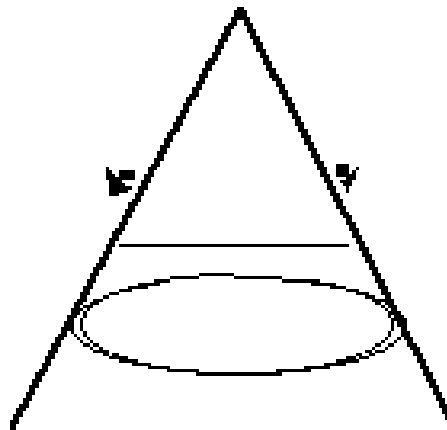


**Figure 3.** Pillon PZM shotgun, with  $2 \times 2$ -ft panels at an angle of  $60^\circ$  to each other. The PZMs are the dark objects outside the angle; the apex of the angle is pointed toward the sound source.

## Details of Electronics

With two digital delay circuits between the microphone elements and a summing amplifier, we can bias the beam to the left or right of the center axis. The high accuracy and precision of available delay circuitry enable us to set the center point of the beam with high precision. Thus, we have a method for scanning along the plane parallel to the base of the Pylon structure that contains the two microphones, without the requirement of physical motion.

A second Pylon assembly located on a parallel plane vertically above the first assembly provides a second beam that we can move in conjunction with the first beam. By electronically delaying these summation voltages prior to a second summation, we can bias the combined beam, thereby defining a plane (actually a hemicylindrical surface) over which the beam traverses with discrete scanning intervals with respect to both the  $x$ - and  $y$ -coordinates.

Calibrating the beams can be done by using a fixed reference source local to the PZM assemblies. A duplicate assembly located at a distance from the first provides a second plane over the area of observation. The intersections of target measurements between these two planes provides us with the third dimension through a change in basis; thus, we are able to detect the outline of an object in the area intersected by the cones bounded by the detection beams and the detection limits of the microphone elements. We use a notch filter with a very narrow bandwidth (a readily available device) and a computer controller in conjunction with the delay circuits to search selectively for any frequency within the limits of the microphone element range. Initially, we propose 1,500 Hz as a reasonable tradeoff between selectivity and sensitivity, but nothing in the mechanism or model requires this particular frequency in preference to any other. We suggest empirical analysis to determine which frequencies produce optimal results in real-world application.

The use of phase cancellation limits the arc angle of the scanning planes. This limit is more practical than theoretical, but realistically we cannot expect to achieve viable cancellations with delays in excess of a single wave period. Beyond this limit, we are faced with superposition problems, including accounting for the reflections from the boundary as they interact with incoming wavefronts. This means that the effective scanning area is limited by the choice of frequency, the sensitivity of the microphone at the selected frequency, and the quantization of the planar grid required for sufficient object resolution. Closer objects will be “fuzzier” but easier to range. Higher frequencies will improve image definition, but at the expense of range. If we are willing to complicate the detection apparatus, we can defer the selection of tradeoff criteria until measurement time. With this approach, we include motors that can vary the angles between the boundary planes and vary the orientation of the two scanning planes by rotating the vertical assemblies about the vertical axis. We can address the frequency characteristics by simultaneously processing several frequencies through a distribution amplifier and a set of narrow notch filters. The complete apparatus can be generalized as shown in **Figures 4 and 5**.

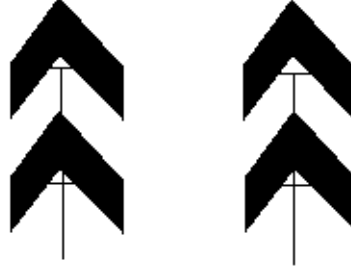


**Figure 4.** Detection array.

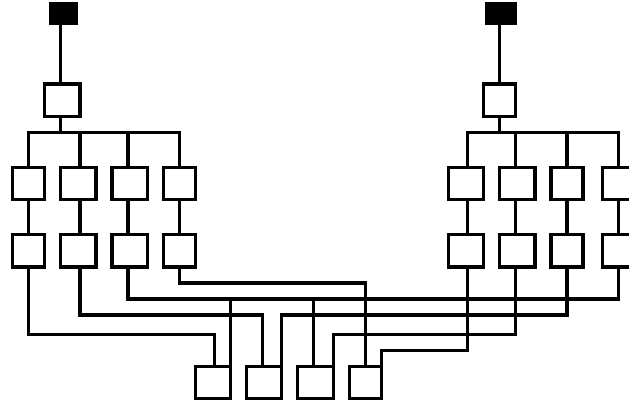


**Figure 5.** Electronic configuration.

Whether we exploit the characteristics of the boundary microphones or instead rely on conventional directional microphones, the scanning equations are identical. There are two factors of concern, the arrival time differential and the amplitude difference. We compute these as follows [Bartlett 1991, 44–45]:

$$\Delta T = \frac{\sqrt{D^2 + \left[\frac{S}{2} + D \tan \theta_s\right]^2} - \sqrt{D^2 + \left[\frac{S}{2} - D \tan \theta_s\right]^2}}{c},$$

where

$T$  is the time differential between the microphones,

$\theta_s$  is the desired source angle,

$S$  is the spacing between the microphone elements,

$c$  is the speed of sound, and

$D$  is the distance from the microphones to the detection plane (the median of the depth plane).

Amplitude signals must be adjusted between the incident pairs in order to flatten the scanning plane. By weighting the amplitude values between the pair, we essentially eliminate the distance factor from the measured sector, which is

appropriate since we compute distance via triangulation rather than absolute amplitude. The amplitude difference in decibels between the two microphones of each pair is

$$\Delta = 20 \log \left[ \frac{a + b \cos \left( \frac{\theta_m}{2} - \theta_s \right)}{a + b \cos \left( \frac{\theta_m}{2} + \theta_s \right)} \right],$$

where  $\theta_m$  is the angle between the boundary planes (or between the microphone elements, in the case of directional elements), and  $a$  and  $b$  are constants that define the polar characteristics of the microphone elements.

There are several possible methods to image the three-dimensional target using our methods.

- We could try to use one additional convergence operation and scan both planes synchronously. This would yield sound pressure levels at points in three-space; in other words, it would result in a parallelepiped field of observation, demarcated by a grid on two of its faces, with pressure readings for each three-dimensional segment. This would yield the best image, but we are concerned that we are asking too much of the convergence techniques.
- We could determine the center of the target in each of the two observation planes and then find the distance to the center of the object using a simple triangulation (since we know the distance between the detection arrays and both angles of detection).
- We could apply a change of basis to one of the planes to map it onto the three-space coordinates of the other, weigh the measurements in the rotated plane by their  $z$ -coordinate values, and add the contents of the matrices. This would yield a two-dimensional matrix whose elements contain a value that should be proportional to the locations depth in the  $z$ -plane. A simpler interpretation of this is that we are intersecting the cylinder formed by extending the two-dimensional shape in each of the observation planes and interpreting this bounding shape as the shape of the object itself. This is more than sufficient image resolution given the limits of the arc formations. By summing the matrices derived from each frequency observed, we should get a reasonably detailed image with this method.

## Deriving Object Characteristics from Data

### Edge Detection

Through the array of hydrophones, we can construct a three-dimensional description of the target. By phase cancellation, we can construct precise narrow cones from the directional hydrophones and effectively orient them in an arbitrary direction. Each cone measures the sound intensity of a point in space, and we can represent this by a value in a two-dimensional matrix. By varying



the delay time, we can sweep the detector field across the plane representing the field of observation; and thus we construct a two-dimensional grid. Each element of the matrix contains the data for the sound intensity of a particular position in space. Since the submarine blocks out the ambient noise, we detect a decrease in sound intensity in the positions of the submarine relative to its surrounding space. This gives us an outline of the submarine in two dimensions relative to the perspective angle of the microphone array (**Figure 6**).

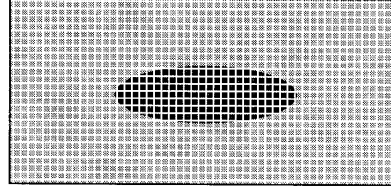


**Figure 6.** Plane scanned by an array of microphones. The dark region indicates the change in sound intensity level relative to the surrounding space, yielding the outline of the submarine.

From a single array of microphones, we cannot obtain the third dimension (the depth) of the submarine; therefore, the model proposes that another array of microphones be oriented at a slight angle to the observation plane and thereby obtain another two-dimensional view of the submarine relative to the perspective angle of this new array, which we call array2.

Knowing the distance between the two arrays of microphones and the angles of their respective planes of observation, we can determine the intersection set of any given set of values—that is, we can locate the same subfield in three-space by deriving the third spatial vector of the first plane from the two vectors (representing the  $x$ - and  $y$ -coordinates) of the second plane. Thus, we can determine the absolute location of the sound field depression in three-space.

## Distance of scanned plane from the microphones

Referring to **Figure 7**, we observe that by the law of sines we have

$$\frac{\sin \beta}{b} = \frac{\sin(180^\circ - \alpha - \beta)}{a} = \frac{\sin \alpha}{c},$$

so that

$$b = \frac{a \sin \beta}{\sin(180^\circ - \alpha - \beta)}, \quad c = \frac{a \sin \alpha}{\sin(180^\circ - \alpha - \beta)}.$$

## Size of each grid box

From **Figure 8**, we see that the area of each grid point is simply the area of the circles traced out by the cone. The radius of the circle is  $r = D \sin \theta$ , so the area of each grid box is  $A = \pi(D \sin \theta)^2$ , where  $D$  is the distance from

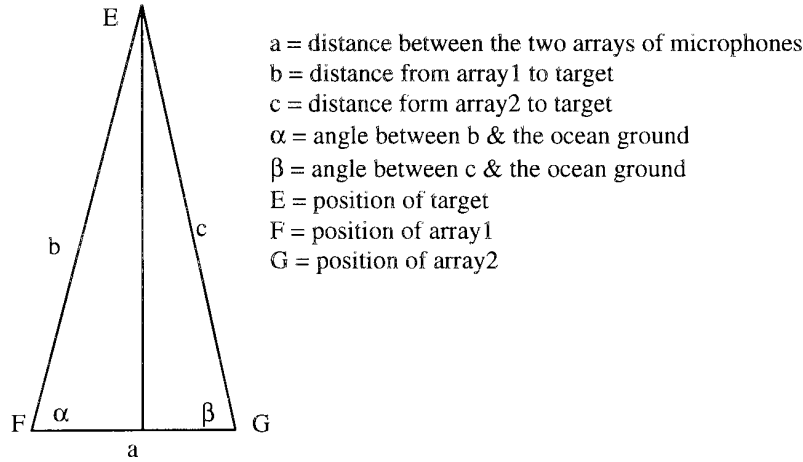


Figure 7. Geometry of microphone arrays.

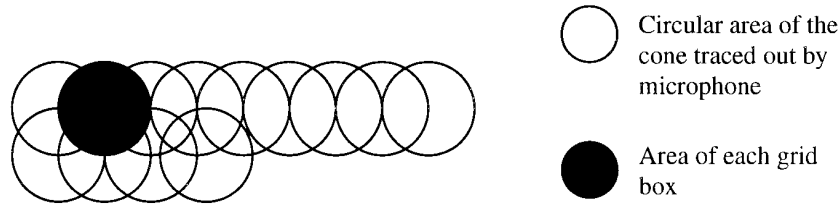


Figure 8. Geometry of grid boxes.

the microphone to the target and  $\theta$  is the angle subtended by the cone of the microphone.

Since the two arrays of microphones are pointed in different directions in space, we have two different directional bases to work with. From array 1, we have a basis with unit vectors  $X_1$ ,  $Y_1$ , and  $Z_1$ ; and each point of the plane represented by array 1 is expressed in terms of this basis with  $X_1$  as the horizontal direction of the plane,  $Z_1$  as the vertical direction of the plane, and  $Y_1$  as the depth, perpendicular to the plane. Similarly, each point on plane 2 represented by array 2 will be expressed in terms of the basis with respect to array 2. Looking at the two planes separately, we cannot determine the  $y$ -component of the picture in either case. Now, if we perform a change of basis for the second plane, we can obtain the depth of the submarine in terms of the first basis. This can be done simply by multiplying the coordinates of each of the points on plane 2 by the matrix

$$\begin{bmatrix} \cos \phi \cos \theta & -\sin \theta & -\sin \phi \cos \theta \\ \cos \phi \sin \theta & \cos \theta & -\sin \phi \sin \theta \\ \sin \phi & 0 & \cos \phi \end{bmatrix},$$

where  $\theta$  is the angle between  $X_2$  (unit vector in the  $x$ -direction of array 2) and the  $X_1 Z_1$ -plane, and  $\phi$  is the angle between  $X_2$  and the  $X_1 Y_1$  plane. Here we are assuming that the distance between the two microphone arrays is significantly small compared to the distance between the submarine and the microphone

arrays; therefore, we have the same origin for both bases and can use this single matrix to perform the change of basis. After the transformation of basis, we obtain the  $Y_1$ -components for each scanned point  $(X_{1i}, Z_{1j})$  on plane 1. Thus we have constructed a three-dimensional “portrait” of the submarine; the location of each of its points is expressed with respect to the basis defined by `array1`.

Now we define a standard basis with respect to the ocean. That is, we use the plane of the bottom of the ocean as the  $xy$  plane and the altitude of the ocean as the  $z$ -axis. We now transform every point in the  $X_1, Y_1, Z_1$  basis into the defined standard basis and obtain an “upright” three-dimensional figure of the submarine. By doing the transformation of the bases in real time on the computer, we can generate a three-dimensional continuous moving shadow of the submarine.

## Size Computation

From the three-dimensional view, we can extract the positions of any given surface point. Hence we can compute the length and width of the submarine. Better yet, we can determine the volume of the ship by summing up all the grid space taken up by the submarine.

## Velocity and Direction

To calculate the velocity of the submarine, we pick any point on the three-dimensional graph and locate its position at time  $t$  and then again at time  $(t + \Delta t)$ , then divide changes in each direction to find the components of the velocity.

## Fun with Microphones

We experimented to test our model of how the submarine would affect the ambient field. Not having a large body of water, we did an air-based experiment. To simulate the ambient noise field, we used speakers connected to a noise generator. Since we did not have a large number of speakers to simulate the entire ambient noise field, we tried several representative orientations of speakers and detector. Our entire set of equipment was

- noise generator,
- amplifier,
- two speakers,
- sound-level meter,

- rolling trash can, and
- small table.

We set up the equipment in several different orientations. For each setup, we took several readings at each location to get an idea of the uncertainty of measurements. Our results are summarized at the end of this section.

In each setup, we pointed the detector directly toward the far noise source  $c1$  (speaker 1) and took readings at three submarine positions  $A$ ,  $B$ , and  $C$ . In every setup, the submarine in location  $A$  has a negligible effect on the ambient field.

**Figure 9** shows the first setup, to simulate the noise field from the opposite side of the submarine, with the noise field from the detector side reflecting off the submarine back toward the detector.

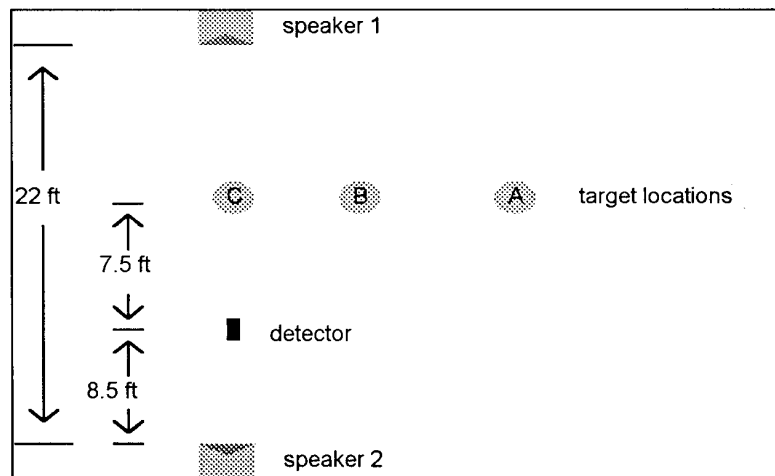


**Figure 9.** Setup 1.

**Figure 10** shows the setup with the sources off to an angle behind the detector so as to measure the reflection of the ambient field off the submarine.

**Figure 11** shows the sources at an angle in front of the detector, to get the opposite of the second setup. By combining the data from both the second and third setups, we hoped to get an idea of the difference between the magnitude of reflection from the submarine and absorption by the submarine.

**Figure 12** is similar to **Figure 11** but with much greater distance to the detector (approximately two and a half times the distance for setup 3).

**Table 1** summarizes our findings for the experiments. We decided that any measured change with an uncertainty greater than the change was not significant. In setup 1, the difference in the ambient field between the submarine in location  $A$  and in location  $B$  was negligible, whereas the difference between the submarine in location  $A$  and in location  $C$  was readily detectable. In the ocean, this would correspond to a measurable decrease in the ambient field when the array is directed toward the submarine, whereas when the array is pointed a little away from the submarine, the submarine would not be detected (i.e.,

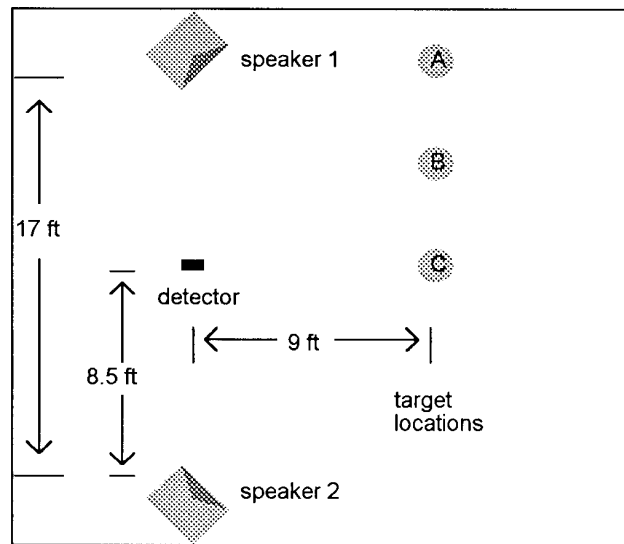


Figure 10. Setup 2.

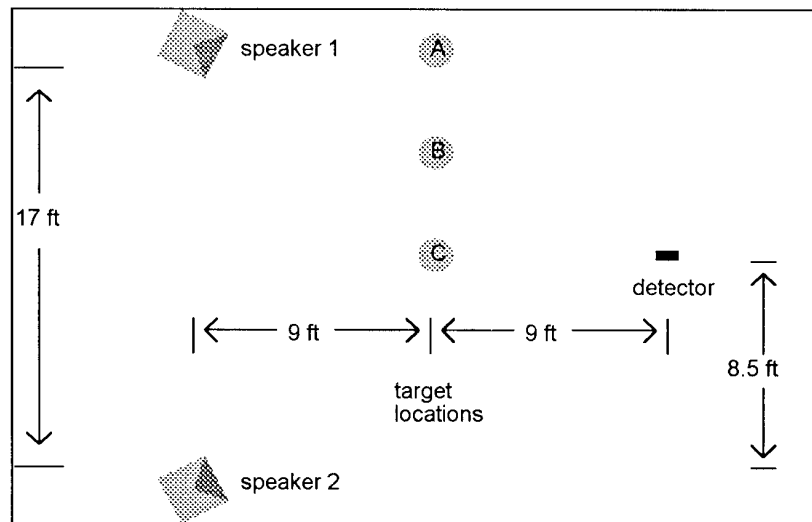


Figure 11. Setup 3.

**Table 1.**  
Results of the experiment.

Setup	Change (in dB) between	
	<i>A</i> and <i>B</i>	<i>A</i> and <i>C</i>
1	not significant	$-1.34 \pm 0.16$
2	not significant	$+0.54 \pm 0.27$
3	$-2.20 \pm 0.23$	not significant
4	$-1.04 \pm 0.25$	not significant

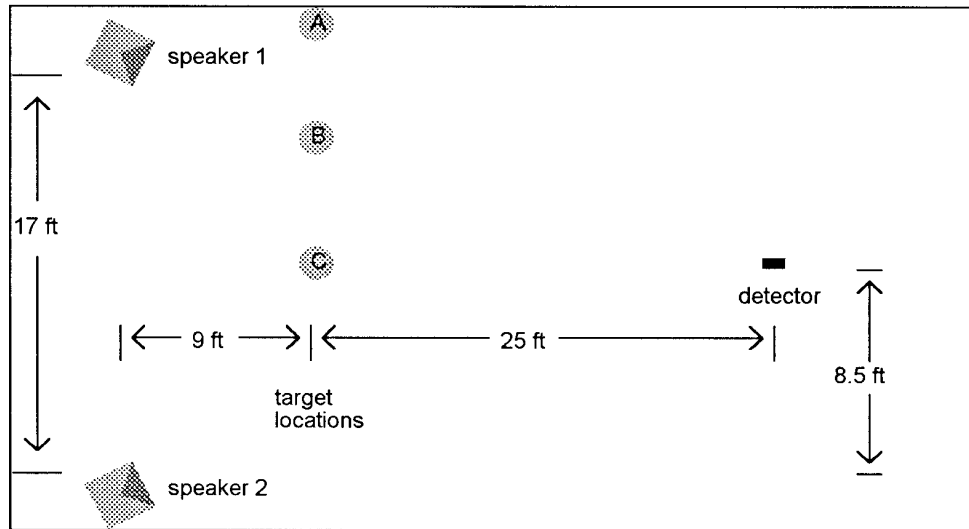


Figure 12. Setup 4.

ambient noise coming off-axis onto the submarine has a negligible effect). This conclusion is corroborated by the data in setups 3 and 4: When the submarine was not directly between the source and the detector, it had little effect on the ambient field; when it was directly between the source and the detector, the submarine had a large effect on the field. So, only noise that comes directly through the submarine to the detector is substantially affected.

The data from all four setups show that the reflected noise from the submarine is lower in intensity than the noise absorbed by the submarine. From setup 1 this is direct. From setup 2 in conjunction with 3, we see that sources of the same intensity reflect back to the detector at +0.54 dB, while the submarine interrupts sources at the same distance from the submarine by 2.20 dB. This difference becomes smaller in setup 4 because the detector can now register more of the ambient field, or the submarine takes up less of the detector's field of view. However, it is still detectable at 1.0 dB.

The data corroborate the fundamental idea that the submarine is detectable as an absence of noise in the ambient field.

## Limitations

There are several problems that our model must deal with.

For a wave to "see" the target, that is, be reflected by the target, it must have a wavelength smaller than the target. We assumed that the smallest dimension (length, width, height) of a submarine would be approximately 5 m. Smaller wavelengths might reflect off large fish; however, we are looking at an array of measurements, and from that we will know if the target is submarine size or fish size.

We also want the frequency to be as low as possible, since low frequencies

tend to attenuate in water far less than high frequencies. We can find the lowest usable frequency from the equation  $c = \lambda f$ , where  $c$  is the speed of sound in water (1,500 m/sec),  $f$  is the frequency of the wave, and  $\lambda$  is the wavelength (5 m). We find that 300 Hz is the lowest optimal frequency. There are other considerations, however. The directionality of the hydrophone array is highly frequency-dependent; in that case, the higher the frequency, the more directional the array can become. We decided that a frequency of 1,500 Hz would not attenuate too much for the additional directionality.

We also find that there is a maximum distance at which we can detect the submarine, even under conditions of ambient noise with fixed frequency and amplitude. The passive sonar equation,

$$SL - TL = NL - DI + DT,$$

can be solved to find the maximum distance. Note that for detection of a submarine in an ambient noise field,  $(NL - SL)$  is the relevant noise relation term. This is the ratio of noise that the submarine will absorb (SL) to the ambient noise level (NL). Rearranging, we get

$$TL = NL - SL - DT + DI.$$

From Urick [1983, 385], we have

$$DT = 5 \log \left( \frac{dw}{t} \right),$$

where  $d$  is a parameter relating the probability of detection and the probability of false alarm,  $w$  is the frequency range, and  $t$  is the length of time listening for the submarine. From Urick [1983, 23], we have

$$DI = 10 \log \left( \frac{P_{\text{equiv}}}{P_{\text{actual}}} \right),$$

where  $P_{\text{equiv}}$  is the noise power generated by an equivalent nondirectional hydrophone and  $P_{\text{actual}}$  is the noise power generated by the actual hydrophone. Another way of looking at this is in terms of the relative area of detection for a nondirectional hydrophone compared to the actual array of hydrophones, so an equivalent equation is

$$DI = 10 \log \left( \frac{\text{surface area of } 360^\circ \text{ scan}}{\text{surface area of actual scan}} \right).$$

Since the arclength of a section on a sphere is given by  $s = r\phi$  for angle  $\phi$  measured in radians, and since for small  $\phi$  the arclength  $s$  is approximately equal to the diameter of the circle inscribed on the sphere, we get the surface area of the scan as

$$A = \pi \left( \frac{r}{2\phi} \right)^2.$$

So we have

$$\text{DI} = 10 \log \left( \frac{4\pi r^2}{\pi \cdot \frac{r^2}{4} \cdot \phi^2} \right) = 10 \log \left( \frac{16}{\phi^2} \right) = 12 - 20 \log \phi.$$

Finally,

$$\text{TL} = 20 \log r + (\alpha \times 10^{-3}) r,$$

with  $\alpha$  given by [Urlick 1983, 108] as

$$\alpha = \frac{0.1f^2}{1+f^2} + \frac{40f^2}{4.100+f^2} + 2.75 \times 10^{-4} \times f^2 + 0.003,$$

for  $f$  expressed in kHz [Urlick 1983, 108]. For our purposes, we neglect the term involving  $\alpha$ .<sup>1</sup>

Using these values, we can now solve for  $r$  as

$$\log r = .05 \left( \text{NL} - \text{SL} - 5 \log \left( \frac{dw}{t} \right) + 12 - 20 \log \phi \right).$$

Included as an appendix are graphs for a perfectly absorbing submarine of range vs. time (**Figure 13**), and, given a sweep time of 1 second, range versus  $\phi$  and  $(\text{NL} - \text{SL})$  (**Figure 14**). Notice that if the submarine is not perfectly absorbing, it quickly becomes hard to detect. For example, recall that the difference between the ambient noise field alone and the field with the submarine present is  $-20 \log a$ . For  $a = .1$ , we have a difference of 20 dB. If this is the case, the submarine is detectable only within 1 km or less, even with a low angle of observation. We can adjust for this somewhat with a slower scan; changing from 1 sec to 3 sec would almost double the range limit for detection. However, the better the absorption factor of the submarine, the easier for us to detect. This implies a tradeoff between absorption for active sonar and reflectivity for passive sonar.

The uncertainty in successive readings limits the smallest noise difference that we can detect, lowering the range limit by approximately the standard deviation of the noise. A reference deviation of a hydrophone is 0.5 dB [Wagstaff and Baggeroer 1985].

There is variation in the amplitude of the ambient field. If the variation is 7 dB, any difference of 7 dB may be insignificant random noise; again, this lowers the range limit by this deviation level. That is, it will lower the effective  $(\text{NL} - \text{SL})$  difference. A common standard deviation in the ambient noise field over one-hour periods is about 6 dB, which results from changing wind speed

---

<sup>1</sup>AUTHORS' NOTE: The relative size of the  $\alpha$ -term depends on the frequency used. Either we see the object or we don't, and some variation in TL is negligible with respect to both detection and imaging. At our suggested frequency of 1500 Hz, and at a range of 3 km, the  $\alpha$ -term is about 38% of the total. But our proposed apparatus could use arbitrarily low frequencies. At 200 Hz (probably a practical minimum), the effect of the omitted term at a range of 10 km is only 5% of the total.



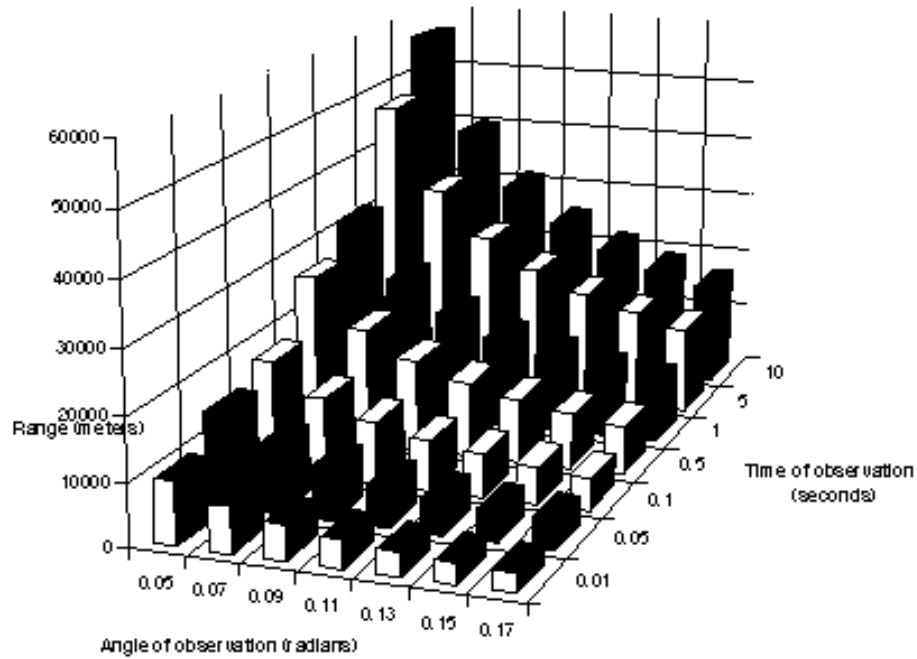


**Figure 13.** Range vs. time of observation and vs. angle of observation.

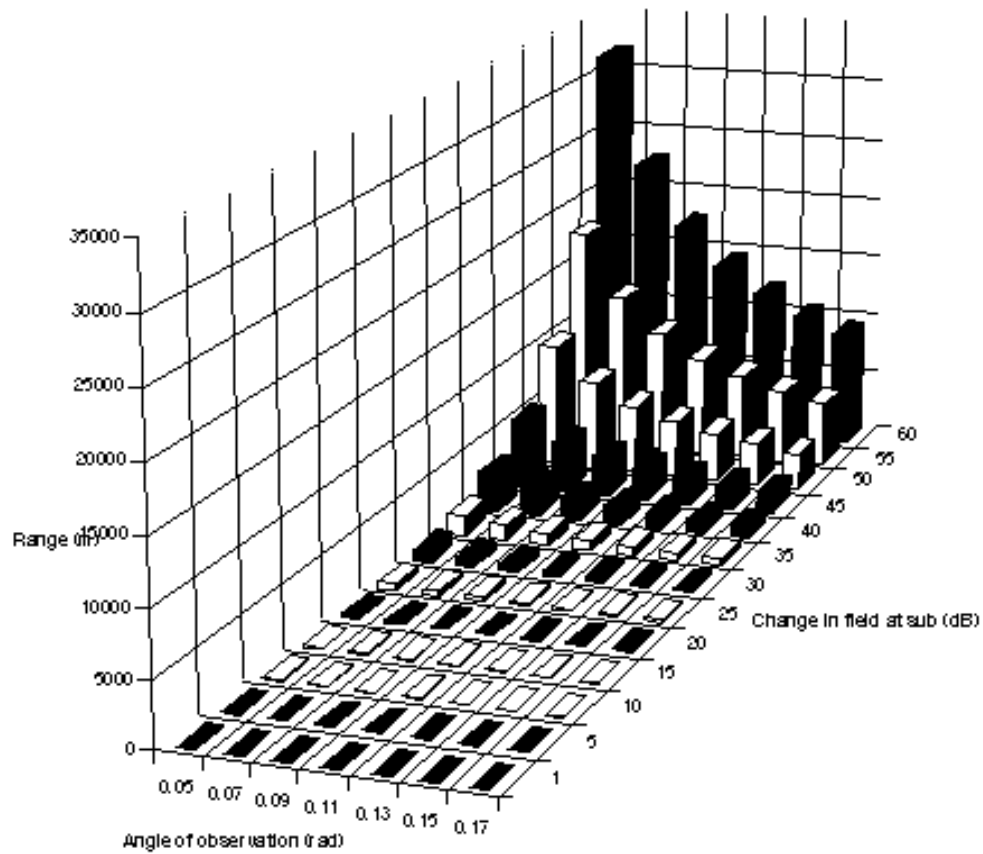


**Figure 14.** Range vs. change in field with reflection and vs. angle of observation.

during the observing period [Urlick 1983]. However, we postulate that the deviation over one- or two-second intervals would be far lower, as the wind speed change would be far less. A reasonable assumption would probably be about 1–2 dB.

We can get around these deviations to some extent by taking a lot of data. That is, if on several successive scans we find a deviation of 1 dB in the same location, it is more likely to be caused by a submarine than by a statistical deviation. Thus, we can probably notice a deviation of less than half the deviation of the ambient noise field or the hydrophone.

A very large problem in positioning the submarine is not directly apparent from our model. The temperature difference at different levels in the ocean combined with pressure gives varying speeds of sound at different depths. While the maximum difference in the speeds of sound between depths of 0 to 1,500 m is only about 10 m/s, a velocity gradient as well as a speed gradient are forced upon the sound wave. This leads to rather strange characteristics in the path of travel of sound (called a ray) in the deep ocean (see Robinson and Lee [1994] and Tucker and Gazey [1966] for pictures of ray tracings).

An interesting note is the fact that a “shadow zone” occurs at some distance from the source. This impacts the placement of the hydrophone; we do not want it in the upper portion of Region II (200–1,500 m) or the lower part of Region I (0–200 m), as these areas are missed by all sound rays at some distance from the source. It also requires some data processing once the location of the submarine has been found. From the equation for the length of an arc, it is easy to verify that

$$\cos \phi_m = \cos \phi_n + \frac{d_n - d}{R_n},$$

where  $\phi_m$  and  $\phi_n$  are the angles of inclination of the incident wave at the detector and at the target, respectively,  $d_n$  is the depth of the detector;  $d$  is the depth of the source; and  $R_n$  is the radius of curvature of the ray path [Tucker and Gazey 1966, 105]. The horizontal distance to the target,  $s_n$ , is given by

$$s_n = R_n(\sin \phi_n - \sin \phi_m).$$

Combining these equations, we can solve for  $d_n$  and  $\phi_n$  if we use the distance to the target computed by the array as  $s_n$ . Of course, this will not be exact, but iterations using  $\phi_n$  to find a new  $s_n$  will give a fairly exact picture. The only problem is when the ray has been reflected by the surface of the ocean or the surface between two regions, or if the ray has gone through more than one region. If this is the case, the actual location of the target is far more difficult to ascertain, and is beyond the scope of this paper.

## Discussion of Alternative Approaches

There are several other methods of detecting the submarine.

One very interesting and purely hypothetical method is the idea of a “sound camera.” This incorporates a sound lens and a nonreflecting box. It works in much the same way as an ordinary camera: It takes the view, inverts it through the lens, and displays it inside the box. This display would probably be in the form of a pressure-sensitive liquid that would have some characteristic change stemming from very small pressure changes and be proportional to those pressure changes. Thus, one would be able to get a “picture” of the sound that the lens is “seeing” by observing the changes in the liquid in the box. Naturally, there are several problems, the foremost being the velocity of sound. Since the velocity of light is essentially infinite with respect to the camera, the entire plane of observation is “seen” at the same time. However, because the speed of sound is very finite, things with distances differing by kilometers or more would be offset in the picture by times of seconds. If they were relatively constant sources, this would not be of much consequence as the source 10 sec before the picture would probably be much the same as the source at the picture. This would be a hard device to design, but it would be very useful in searching the ocean for sound sources. Reconstructing a visual image from the sound field could probably be done using acoustic holography, a technique described below as an additional alternative approach.

A second alternative is a variant on a method described by Farrah et al. [1970] regarding sound holography. They describe the techniques for reconstructing a holographic image using sonar data. Just as a laser can be used to read the pits of a compact disk, or scan the surface of an LP recording, it would be possible for us to “read” the sound waves in water by measuring the refraction of a laser beam passing through them. We would be able to read specific waves from within the compendium of the ambient field, theoretically to any precision. Scanning the plane representing the observation threshold, we could reconstruct a plane parallel to it by subtracting the waves whose source can be determined to be off-axis to the observation plane. Time provides the third spatial dimension, so we should be able to locate and measure a target item within the observation space.

## Conclusion

Our model allows for the prediction of a perfectly absorbing submarine to extreme distances with exceedingly good technology (see **Figure 13**). However, with a more realistic model of a submarine, the detection limit falls to less than 5 km, and possibly less than 1 km. Nevertheless, the array can also detect a submarine generating non-machinery-based noise (such as flow noise and cavitation), so we may hear a quickly-moving submarine at large distances.

## References

- Albers, Vernon. 1965. *Underwater Acoustics Handbook*, vol. 2. University Park, PA: Pennsylvania State University Press.
- Bartlett, Bruce. 1991. *Stereo Microphone Techniques*. Stoneham, MA: Butterworth-Heinemann.
- Cox, Albert. 1982. *Sonar and Underwater Sound*. Lexington, MA: Lexington Books.
- Farrah, H.R., E. Marom, and R.K. Mueller. 1970. An underwater viewing system using sound holography. In *Proceedings of the 2nd International Symposium on Acoustical Holography*, edited by A.F. Metherall and L. Larmore, 173–184. London: Plenum.
- Hassab, Joseph. 1989. *Underwater Signal and Data Processing*. Boca Raton, FL: CRC Press.
- Horton, Joseph. 1957. *Fundamentals of Sonar*. Annapolis: U.S. Naval Institute.
- Metherell, A.F., and Lewis Larmore (eds.). 1970. *Acoustical Holography*, vol. 2. New York: Plenum Press.
- Naval Sea Systems Command. 1984. *Ambient Noise in the Sea*. Washington: Dept. of the Navy.
- Nisbett, Alec. 1974. *The Use of Microphones*. New York: Hastings House.
- Robinson, Allan, and Ding Lee (eds.). 1994. *Oceanography and Acoustics*. Woodbury, NY: AIP Press.
- Tucker, David, and B. Gazey. 1966. *Applied Underwater Acoustics*. London: Pergamon Press.
- Urick, Robert J. 1967. *Principles of Underwater Sound for Engineers*. New York: McGraw-Hill.
- \_\_\_\_\_. 1982. *Sound Propagation in the Sea*. Los Altos, CA: Peninsula Publishing.
- \_\_\_\_\_. 1983. *Principles of Underwater Sound*. 3rd ed. New York: McGraw-Hill.
- Wagstaff, Ronald, and Arthur Baggeroer (eds.). 1985. *High-Resolution Spatial Processing in Underwater Acoustics*. NSTL, MS: Naval Ocean Research and Development Activity.
- Wilson, Oscar. 1985. *An Introduction to the Theory and Design of Sonar Transducers*. Washington: U.S. Government Printing Office.